



Swansea University
Prifysgol Abertawe



Cronfa - Swansea University Open Access Repository

This is an author produced version of a paper published in:

Thermology International

Cronfa URL for this paper:

<http://cronfa.swan.ac.uk/Record/cronfa40808>

Paper:

Malik, T., Clement, R., Gethin, D., Krawszik, W., Parker, A. & Thomas, R. (2015). Infrared study of dew harvesting cacti spines. *Thermology International*, 25(1), 7-13.

This item is brought to you by Swansea University. Any person downloading material is agreeing to abide by the terms of the repository licence. Copies of full text items may be used or reproduced in any format or medium, without prior permission for personal research or study, educational or non-commercial purposes only. The copyright for any work remains with the original author unless otherwise specified. The full-text must not be sold in any format or medium without the formal permission of the copyright holder.

Permission for multiple reproductions should be obtained from the original author.

Authors are personally responsible for adhering to copyright and publisher restrictions when uploading content to the repository.

<http://www.swansea.ac.uk/library/researchsupport/ris-support/>

Infrared study of dew harvesting cacti spines

Malik FT¹, Thomas RA⁴, Clement RM¹, Gethin DT³, Krawszik W¹ and Parker AR²

tegwenmalik@hotmail.com & roderick.thomas@wales.ac.uk

¹The Institute of Life Science, College of Medicine, Swansea University, Swansea, SA2 8PP, UK

²Department of Life Sciences, Natural History Museum, Cromwell Road, London, SW7 5BD, UK

³College of Engineering, Swansea University, Swansea, SA2 8PP, UK

⁴University of Wales Trinity Saint David, Mount Pleasant Campus, Swansea, SA1 6ED, UK

Summary

The focus of this study was to gain further understanding on the thermodynamic behaviour of the dew and non-dew harvesting spines of cacti. Four species of cacti were chosen, three that were known to harvest dew on their spines and one that does not. The temperature gradient of the spines of the most efficient dew harvesting species, *Copiapoa cinerea* var. *haseltoniana*, and the IR emissivity of the cactus spines for all four species were determined. When placed outdoors, around the hours of sunrise and sunset, the tips of the spines of *C. cinerea* appeared constantly warmer than their base or mid-sections, even during the cooling hours of sunset. Also, the IR emissivities of the spines of the three dew harvesting cacti were higher than those of *Ferocactus wislizenii*, the cactus species which does not harvest dew. The highest spine IR emissivity was recorded for *Mammillaria columbiana* subsp. *yucatanensis* at 0.98 ± 0.016 followed by *C. cinerea* and *Parodia mammulosa* with IR emissivities of 0.97 ± 0.007 and 0.93 ± 0.004 respectively. *F. wislizenii*, which does not harvest dew on its spines, was found to have the lowest spine emissivity of 0.89 ± 0.009 .

Keywords: thermography, water harvesters, dew, cacti, emissivity, infrared

Introduction

This study forms part of a broader investigation looking into the possibilities of translating nature's own methods for harvesting airborne moisture into a biomimetic moisture harvesting device. Here, infrared (IR) measurement was used to gain further understanding into the formation of dew on the surface of some of nature's known dew harvesters (in this case cactus spines), since dew forms only on surfaces cooled below the dew point temperature. Four species of cacti were studied, three known to harvest dew on their spines and one that is known not to do so. Two of the three dew harvesting cacti, *Mammillaria columbiana* subsp. *yucatanensis* and *Parodia mammulosa*, were part of a previous study on dew harvesting cacti (i.e. prior exploratory investigations carried out during dewy weather in the UK), the third, *Copiapoa cinerea* var. *haseltoniana* was also part of this study but had additionally been reported in the literature to have dew harvesting capability [1]. The last of the four species, *Ferocactus wislizenii*, was likewise observed in this study but was chosen as a comparative species, with Shreve (1916 cited in Nobel [1]) finding it not to harvest airborne moisture on its spines.

The aim of this paper was to study the thermal response of the cactus spines during sunrise and sunset, using thermal imaging cameras to gain insight into the dew harvesting mechanisms and to further determine the emissivity of the spine surfaces.. Cone shaped structures, such as cactus spines, have previously been identified as an important structure for harvesting airborne moisture [2]; it was thus

deemed important to assess the spines in detail, using thermographic analysis to study their temperature gradient. Infrared Thermal Imaging (IRT) has previously been used to study plants and the nucleation of ice or frost on their surfaces [3-5] as well as signs indicating plant stress [6, 7] but not, to our knowledge, with regard to dew formation.

Object emissivity values lie within the range of 0 to 1.0, with 1.0 being highly emissive and corresponding to that of a blackbody and 0 having no infrared energy emission. The emissivity of cacti has been reported in the literature for several different species, with values of at least 0.96 in a study of eight cactus species [8-10] but no figure for emissivity has been assigned to cactus spines *per se*. Establishing this was one of the principal aims of this study.

Methodology

The methodology chosen was, firstly, to analyse the temperature gradient along a spine of the most efficient dew harvesting cactus, *C. cinerea*, by capturing temperature gradient data for the spine observed outdoors during the hours of sunrise and sunset. The second element of the methodology utilised a climate chamber to maintain a stable environment to measure the IR emissivity of cactus spines for three species known to harvest dew and to compare these emissivities with that of the species of cactus whose spines do not harvest dew.

Thermographic data was captured using the Longwave Optris PI450 Infrared Camera to collect temperature data for the cactus spine of *C. cinerea* when placed outside around the hours of sunset and sunrise. The IR camera used had a spectral range of 7.5 to 13 μ m, enabling detection of infrared wavelengths whilst minimising atmospheric absorption and, as a consequence, increasing detail. The camera had a detector resolution of 382 x 288 pixels, frame rate of 80 Hz and a system accuracy of $\pm 2^{\circ}\text{C}$. The thermal sensitivity varied depending on which lens was used. For the 13 $^{\circ}$ lens, the temperature resolution was 0.06K and for the 38 $^{\circ}$ lens, the lens of choice for the key elements of this study, it was 40mK. The rainbow thermogram palette (the preferred choice in medicine [11]) was utilised throughout this study to provide a visual indication of the temperature (warmer areas are red and the cooler areas are blue).

Temperature gradient of individual spines

C. cinerea was placed outside on a night during which dew was likely to form, away from any objects such as buildings or trees that would obscure it from having full view of the night sky. This was achieved by placing it on a flat roof on top of a sheet of polystyrene to insulate it from below and raising it, using a plastic container, to a height that enabled the IR camera to focus on the cactus apex. The 38 $^{\circ}$ lens was utilised to maximise the spatial resolution, imaging only the area of the single spine under investigation. Thus highly resolved thermographic data was captured to assess in detail the spine temperature gradient. The material of a spine is the same along its length and it is therefore possible to draw meaningful temperature gradient results using the technique outlined here. Different cacti species cannot be compared with each other unless their emissivity is calculated and used to obtain true temperature readings.

A spine orientated horizontally was selected for monitoring and target measurement areas were identified and positioned using the software to capture the temperature at the base, mid-section and tip of the same spine (Figure (b)). To ensure these target areas were accurately aligned over the area of the

spine in focus and that background thermal data was minimised, a metal rod was used during the set up phase to increase the contrast of the spine against the background, allowing the target measurement area to be positioned accurately.

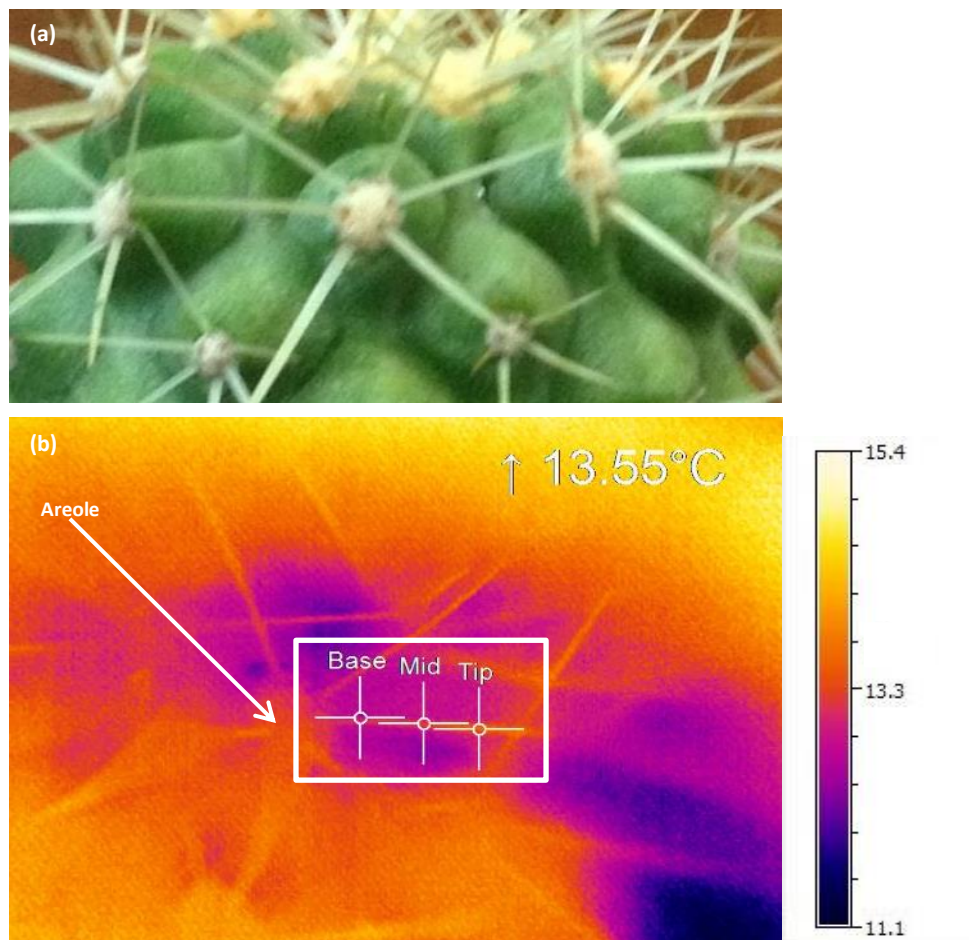


Figure 1: Digital microscope and IR images taken of *C. cinerea*

(a) Digital microscope image of *C. cinerea*; (b) Infrared image of an areole of *C. cinerea* showing the target measurement areas on the spine (highlighted in the white box and showing the target area at the base, mid-section and tip), image is not of the same area as in (a).

The average length of a spine from this plant was measured to be typically $8.6 \text{ mm} \pm 2.7 \text{ mm}$ with an average spine base width of typically $0.4 \text{ mm} \pm 0.08 \text{ mm}$. As the tip of the spine tapered to a point, the measuring area at the tip was not positioned exactly on the spine tip but rather slightly below it, again to ensure no background thermal data was captured due to a larger measuring target area compared to the area of the narrow tip.

The earth's key source of surface energy is the sun's shortwave radiation, with the hours around sunset seeing a cooling of the earth's surface and heating occurring soon after sunrise [12]. Thus the periods around sunset and sunrise were chosen as times of interest for this study. The camera was set to run for one hour between 21:30 and 22:30 hours GMT as the sun was setting on 2 July 2014 (at approximately 21:31 hours GMT) and again for an hour, between 04:50 and 05:50 hours GMT, as the sun was rising on 3 July 2014 (at approximately 05:08 hours GMT).

Emissivity of Cactus Spines

The spines of cacti occur in an array of different shapes, sizes and colours. As a consequence, this study did not generalise and the precise spine emissivity for each of the four species of cactus under investigation was measured, although, spine emissivity was assumed to be constant along a spines

length. The woody nature of the spines was likened to that of tree bark of which emissivity of certain species has been measured, with an average recorded value of 0.95 [13].

The standard method of using a reference material as an aid in measuring the unknown emissivity of a material was employed [14]. Thus a thermocouple attached to a spine on each of the four species under investigation was used as a temperature reference (in the same manner in which a reference material would have been used) from which to compare the IR camera temperature readings at the target measurement area. To ensure that the target measurement area was positioned accurately on the spine and close to but not on the attached thermocouple, a metal rod was utilised once again in the set-up phase, to increase the contrast between the spine and the background. Furthermore, the thermocouple wires were made into a coil shape and wrapped tightly around the spine, ensuring there was good thermal contact with the spine along with adequate thermal mass from which to obtain an accurate temperature measurement from which to be used as a comparative reference. The emissivity settings on the IR camera were then adjusted until the spine temperature displayed on the camera matched the thermocouple temperature reading. Increasing the emissivity of the area in question caused a decrease in the measured temperature for that region [15], the relationship of which is given in Equation 1.1 in the next section.

The measurements were taken at a temperature of 20°C and at 40% relative humidity. The presence of gas, dust, moisture and other atmospheric particles is known to cause absorption and scattering of radiation between the IR camera and the object being imaged [16]. Thus atmospheric attenuation of the measured infrared radiation was minimised by carrying out the measurements in a Sanyo MTH 2400 climatic test chamber to keep dust and moisture particles low by maintaining a low humidity.

Results and Discussion

Outdoor spine temperature gradient experimental results and discussion

Dew was observed to form on the spines of the cacti exposed to the night sky on the night chosen for the test. (i.e. on the planographic surface areas). A thermogram and digital microscope images were captured as shown for *M. columbiana* (Figure 2). Dew droplets can be seen on the spines in both of these images. This led on to the temperature gradient estimate for individual spines being carried out on *C. cinerea* to enable a better understanding of this dew formation.

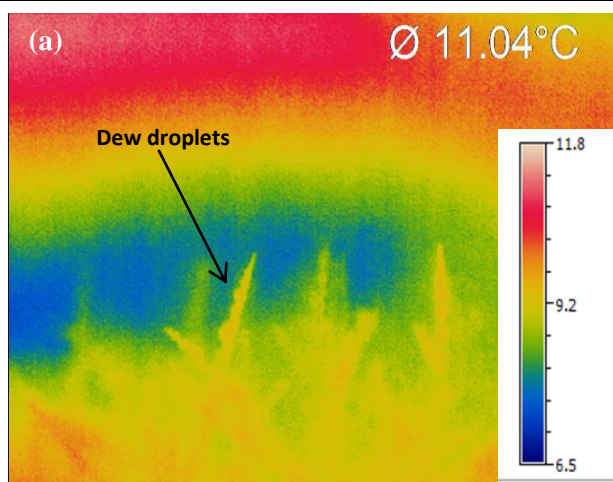


Figure 2: Thermogram and digital microscope image of *M. columbiana* following a dewy night
(a) Thermogram using the 13° lens, clearly showing dew droplets on a spine but no clear thermal difference and (b) the apex of the plant showing the dew that formed during the night.

Following the recording of the thermograms around sunset and sunrise, the temperature-time diagram data was extracted from the images. The temperature at a spine tip, mid-section and base was recorded for *C. cinerea* (see Figure and Figure). This particular species of cacti was chosen as it was found in earlier experiments to be the most efficient at harvesting dew on its surface. It appears that, as expected, the spine cools as the sun sets and warms up as the sun rises..

The temperature differences over an object under investigation can be masked by the temperature achieved due to the heat energy flux variation during the daily cycle. So the hours of sunrise and sunset, during which the solar heat source changes and the temperature differences become evident, were chosen for this study. Equation 1.1 was used to calculate the amount of radiation emitted ($Q_{Emitted}$) from an object during radiative cooling to a background reference of 0K:

$$Q_{Emitted} = \varepsilon\sigma AT^4 \quad \text{Equation 1.1}$$

Where ε is the emissivity of the object, σ is Stefan-Boltzmann constant equal to $5.669 \times 10^{-8} \text{ W/m}^2\cdot\text{K}^4$, A is the surface area of the object and T is the object's absolute temperature. Thus, we hypothesise that the smaller the object's surface area (i.e. smaller tip compared to the wider spine base), the less radiation is emitted from it and therefore the higher its temperature will be.

At sunset the tip of the spine cools more slowly than the mid-section (Figure (a)). This finding is in keeping with Equation 1.1 as well as with 3D simulation results by Fu *et al.* [17] who found that during cooling and for a wind velocity of 0.5 and 2.5 m/s, a cactus spine tip is warmer than its base for both wind velocities (although for the higher wind velocity, the spine was warmer as a whole). A three-second section of the temperature-time data was selected to observe the temperature difference between the three sections of the spines in more detail (Figure (b)). A similar temperature was measured at the base and mid-section of the spine. The base was marginally warmer than the mid-section for the first 10 minutes around the hours of sunset, after which the mid-section became warmer than the base. It is also clear that, as the sun sets, there is no sudden temperature drop in the spine as a whole, with a gradual decrease in the spine temperature and with the tip taking longest to cool. We do not expect this to be due to internal thermal conduction from the body of the cactus to the spine because then the base of the spine would be expected to be warmer, although the plant stem and the arrangement of spines could create a microclimate around each plant. This, along with internal heat transfer, could be of interest in future studies.

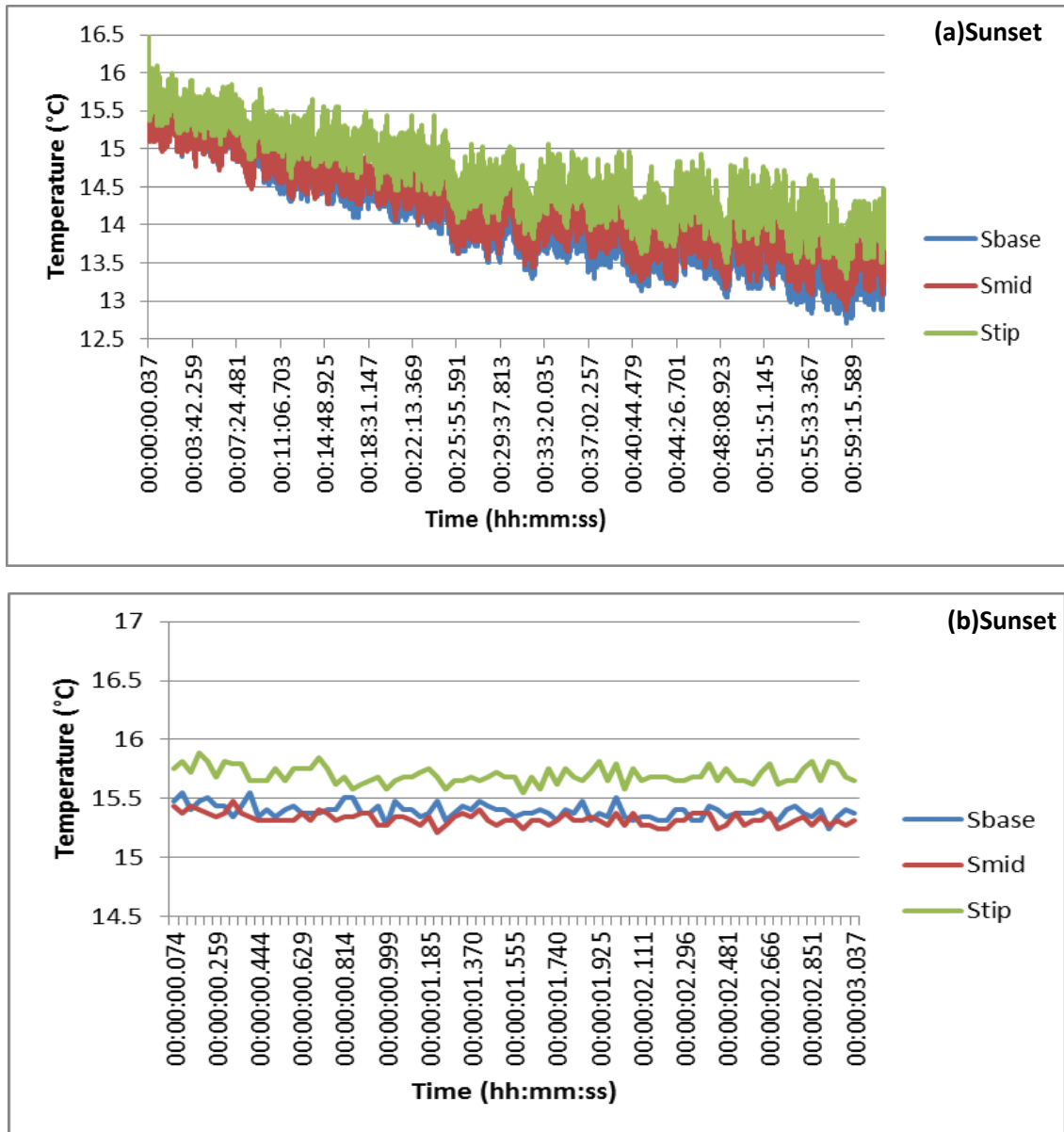


Figure 3: Spine temperature gradients at sunset for *C. cinerea*

The temperature-time graph around sunset with readings for a spine's base (Sbase), mid-section (Smid) and tip (Stip): (a) detailed graph for 1hr 45 minutes around sunset and (b) a three-second section of the detailed temperature-time data.

Around the hours of sunrise (Figure), the tip of the spine warmed most quickly with the base and mid-section recording similar temperatures, and the mid-section recording a slightly warmer temperature than the base overall. During the first few minutes of sunset, similar temperatures were recorded at the tip, mid-section and base albeit the tip was marginally warmer.

The tip was always warmer than the rest of the spine throughout the recorded hours around sunset and sunrise, which could explain why dew droplets were observed forming at the base and mid-sections of the spines before appearing at their tips. The recorded temperature gradient on the spine needs to be taken into account when considering droplet growth, as it is this gradient which could impact on the formation of dew on the spine. That is, the cooler spine areas will have a greater expected rate of condensation. However, even though this temperature difference is real, it is less than a degree, which may not be a significant enough to affect the dew formation rate along the spines.

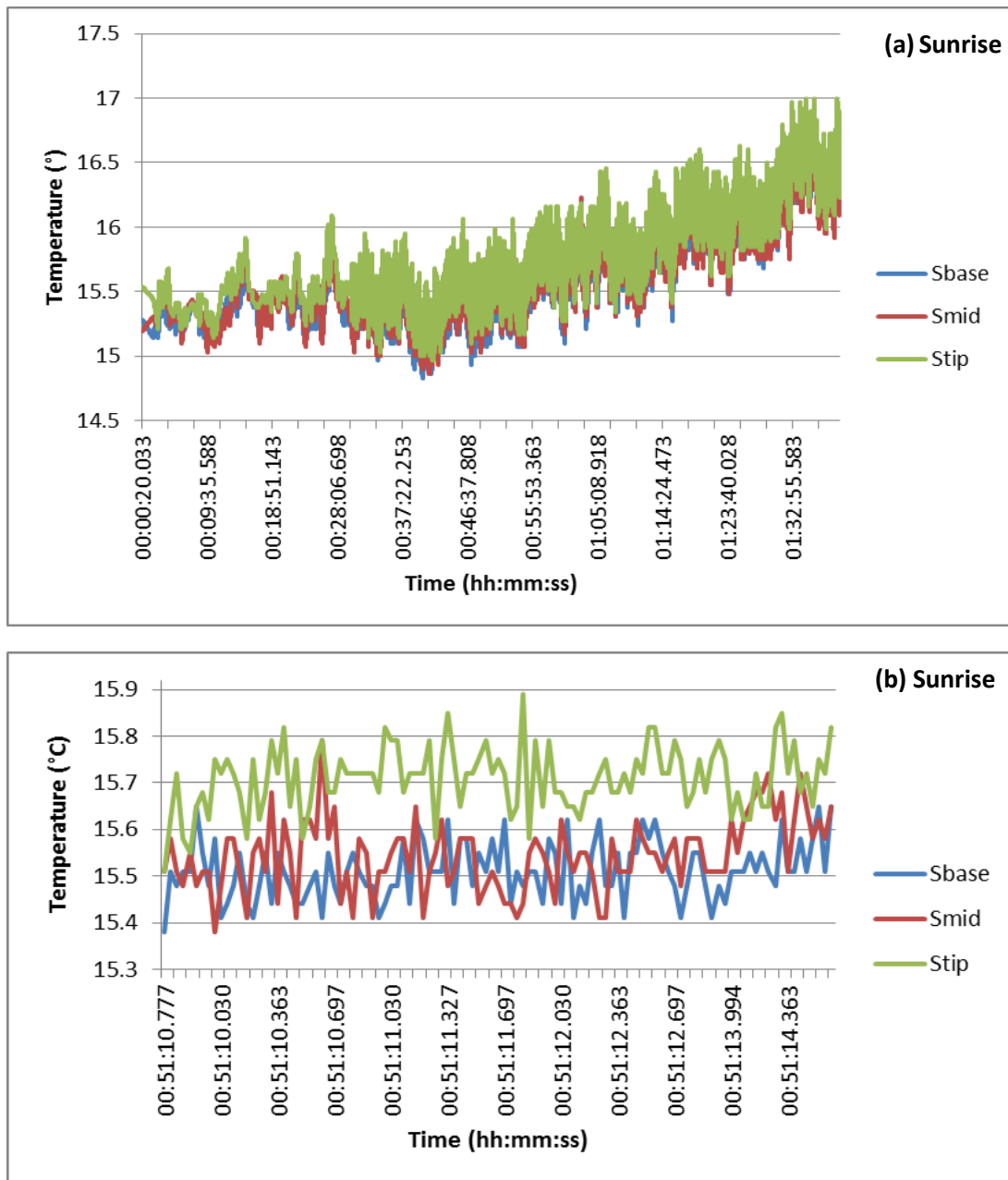


Figure 4: Spine temperature gradients at sunrise for *C. cinerea*

The temperature-time graph at around sunrise with readings for a spine's base (Sbase), mid-section (Smid) and tip (Stip): (a) detailed graph for 1hr 45 minutes around sunrise and (b) detail of a five-second section of the temperature-time data.

Emissivity of Cactus Spines

To facilitate detail thermal analysis, typified by that of Yu *et al.* [17], it is important to gain an accurate determination of the emissivity of the spines since this is absent from the literature. Five measurements were taken from the same point on the same spine (close to but not touching the attached thermocouple reference) of each of the four species in this study. The measurements obtained are given in Table 1, along with the mean (M) and standard deviation (SD). All the spines were found to be highly emissive, with the measurements of *F. wislizenii* found to be the least emissive at 0.89 ± 0.009 . The spine

emissivities of *M. columbiana*, *C. cinerea* and *P. mammulosa* were measured to be 0.98 ± 0.016 , 0.97 ± 0.007 and 0.93 ± 0.004 respectively. The fact the spine emissivity of these four species of cacti are all high, does not explain the absence of dew on the spines of *F. wislizenii* compared to the other species. Other reasons, such as spine surface morphology, could play a role in inhibiting the nucleation of dew droplets on *F. wislizenii* which has a high density of tightly packed microstructures on its surface.

Table 1: Mean spine emissivity for four species of cactus with the five measurements taken at the same point on the same spine (close to the attached thermocouple reference)

Emissivity	<i>C. cinerea</i>	<i>F. wislizenii</i>	<i>M. columbiana</i>	<i>P. mammulosa</i>
Measurement 1	0.963	0.89	0.99	0.93
Measurement 2	0.96	0.893	0.95	0.925
Measurement 3	0.973	0.87	0.98	0.925
Measurement 4	0.975	0.89	0.975	0.933
Measurement 5	0.973	0.89	0.99	0.925
Mean	0.97	0.89	0.98	0.93
St. Deviation	0.007	0.009	0.016	0.004

Whilst carrying out these measurements, all but *F. wislizenii* gave consistent readings on the IR camera and the emissivity of the measuring area could be adjusted until its temperature reading matched the thermocouple reading. Even though the standard deviation of the emissivity measurement for *F. wislizenii* was low, the IR camera gave fluctuating readings for this species, making it problematic to select an emissivity.

It is known that backscattering is increased for rougher surfaces, increasing not only the measured spectral emissivity of an object but also fluctuation in this measurement [18]. Therefore, we suggest that the known surface microstructures on the spines of *F. wislizenii* could have caused the unstable readings on the IR camera. The surface scattering of infrared due to the spine's microstructures is a consideration beyond the scope of this study.

Conclusion

For a single spine of *C. cinerea*, the tip always appeared hottest when placed outside and measured around the hours of sunrise and sunset. It is probable that the tip is warmer when placed outside to cool by nocturnal radiation due to its smaller surface area. These findings are in keeping with the 3D radiative cooling cactus spine simulations carried out by Yu *et al.* [17].

The emissivity of the spines of *F. wislizenii* was found to be the lowest of the four cactus species at 0.89 ± 0.009 . This was the only cactus in this study whose spines did not show any sign of encouraging dew droplets to nucleate on their surfaces. However, even though its spines had the lowest emissivity of the four species, they were still found to be highly emissive. As such, we conclude that the absence of dew nucleation on the spines of *F. wislizenii* cannot be explained by a lower emissivity but must be due to other reasons such as surface morphology.

Even though limitations were found with this technology (i.e. within the optics and the thermal and spatial resolutions of the detector), in general these results indicate that infrared analysis is an important method which can assist in the comprehensive modelling of the moisture harvesting associated with cactus spines..

Acknowledgments

This research paper was funded by Fujitsu and supported by HPC Wales and Swansea University. Thanks are due to The Botanical Gardens in Singleton Park, Swansea, for donating two of the four species of cactus to this research project (*M. columbiana* and *P. mammulosa*) and thanks also to Jenny Childs for her assistance in the generation of this manuscript.

References

1. Nobel, P.S., *Environmental biology of agaves and cacti* 2003: Cambridge University Press.
2. Malik, F., et al., *Nature's moisture harvesters: a comparative review*. *Bioinspiration & biomimetics*, 2014. **9**(3): p. 031002.
3. Fuller, M.P. and M. Wisniewski, *The use of infrared thermal imaging in the study of ice nucleation and freezing of plants*. *Journal of Thermal Biology*, 1998. **23**(2): p. 81-89.
4. Wisniewski, M., S.E. Lindow, and E.N. Ashworth, *Observations of ice nucleation and propagation in plants using infrared video thermography*. *Plant Physiology*, 1997. **113**(2): p. 327-334.
5. Workmaster, B.A.A., J.P. Palta, and M. Wisniewski, *Ice nucleation and propagation in cranberry uprights and fruit using infrared video thermography*. *Journal of the American Society for Horticultural Science*, 1999. **124**(6): p. 619-625.
6. Hatfield, J., *Measuring plant stress with an infrared thermometer*. *HortScience*, 1990. **25**(12): p. 1535-1538.
7. Kebede, H., D.K. Fisher, and L.D. Young, *Determination of Moisture Deficit and Heat Stress Tolerance in Corn Using Physiological Measurements and a Low-Cost Microcontroller-Based Monitoring System*. *Journal of Agronomy and Crop Science*, 2012. **198**(2): p. 118-129.
8. Arp, G.K. and D.E. Phinney, *Ecological variations in thermal infrared emissivity of vegetation*. *Environmental and Experimental Botany*, 1980. **20**(2): p. 135-148.
9. Idso, S.B., et al., *A Method for Determination of Infrared Emittance of Leaves*. *Ecology*, 1969. **50**(5): p. 899-902.
10. Smith, M.W., *Effect of infrared reflectance on stem temperatures of saguaros*. 1989.
11. Ring, E., *Beyond human vision: the development and applications of infrared thermal imaging*. *The Imaging Science Journal*, 2010. **58**(5): p. 254-260.
12. Enz, J.W., V. Hofman, and A. Thostenson, *Air Temperature Inversions*. 2014.
13. Salisbury, J.W. and D.M. D'Aria, *Emissivity of terrestrial materials in the 8–14 μm atmospheric window*. *Remote Sensing of Environment*, 1992. **42**(2): p. 83-106.
14. ISO, *Condition monitoring and diagnostics of machines – thermography – part 1: general procedures*. 2008.
15. Huda, A.N., S. Taib, and D. Ishak. *Analysis and prediction of temperature of electrical equipment for infrared diagnosis considering emissivity and object to camera distance setting effect*.
16. Thomas, R., *IR Handbook: An informative guide for the use of thermal imaging cameras*, 1999, Coxmoor Publishers.
17. Yu F., et al., *SIMULATION DE CONDENSEURS RADIATIFS DE ROSEE: Internal Report*, 2014.
18. Wang, Z.W., et al., *Microstructure and infrared emissivity property of coating containing TiO₂ formed on titanium alloy by microarc oxidation*. *Current Applied Physics*, 2011. **11**(6): p. 1405-1409.